

Time integrating optical signal processing

P. Kellman

ESL, Incorporated
495 Java Drive
Sunnyvale, California 94086

Abstract. Time integrating acousto-optic processors realize flexible, multipurpose complex signal processing architectures based on correlation algorithms. One- and two-dimensional techniques are presented including examples of spectral analysis and ambiguity function processing. Noncoherent optical processor implementation using interferometric detection with electronic reference is described and experimental results are given.

Keywords: acousto-optics, signal processing, correlators, spectral analysis, ambiguity function, triple-product processor, chirp algorithm.

Optical Engineering 19(3), 370-375 (May/June 1980)

I. INTRODUCTION

Optical techniques for linear signal processing lend themselves naturally to large time-bandwidth product operations due to the high degree of parallelism found in optical systems. Parallel optical signal processing has traditionally exploited spatial integration^{1, 2} to realize functions such as filtering and spectral analysis. In this manner, the potential time-bandwidth product, or number of cycles integrated, is proportional to the large number of degrees of freedom of the optical system, though a practical limitation is imposed by input and output devices such as light modulators and detectors.

Integration in time rather than space may be used to realize extremely large time-bandwidth products. Time integrating techniques have recently been generalized for one- and two-dimensional complex signal processing.³⁻⁵ Interest in time integrating techniques has resulted due to the attractive device technology as well as flexibility of time integrating algorithms. An important consequence of time integrating techniques is the ability to operate on signals with very large time-bandwidth product without having to store the entire time history as a spatial record. Therefore, an important class of two-dimensional and multichannel processing algorithms may be performed without requiring two-dimensional spatial light modulators. Acousto-optic devices and charge coupled image sensors are particularly well suited for time integrating processor implementation. Further, these signal processing techniques may be realized with either coherent or noncoherent optical systems.

The optical signal processing architectures discussed in this paper are based on acousto-optic or other traveling wave input modulation devices. Time integrating optical correlators were first demonstrated using translating optical masks,⁶⁻⁹ and scanning detector systems.^{7, 10} In signal recording applications, time integrating techniques have been used to compensate Doppler shift.^{11, 12} Time integrating correlator implementation has been demonstrated using acousto-electric surface wave technology.¹³ Acousto-optic implementations of one-dimensional time integrating correlation and spectral analysis have first been introduced by Montgomery,¹⁴ Sprague, and Koliopoulos.¹⁵ Two-dimensional time integrating techniques were introduced by Kellman^{3, 4} and Turpin.⁵ In this paper, time integrating acousto-optic signal processing is reviewed, and the concept of interferometric detection with electronic reference is described. These techniques are generalized for complex computation, and examples of spectral analysis and ambiguity function processing are given.

This paper is organized as follows. Time integrating correlation

Original manuscript OD-213 received November 12, 1979.

Accepted for publication December 3, 1979.

This paper was presented at the SPIE seminar on Acousto-Optic Bulk Wave Devices, November 27-29, 1979, Monterey, California, and appears in: SPIE Proceedings Volume 214.

©1980 Society of Photo-Optical Instrumentation Engineers

is reviewed in Section 2 and interferometric implementation with electronic reference is described. Time integrating spectral analysis by means of the chirp algorithm is described in Section 3, and the experimental result of a noncoherent optical implementation is given. Two-dimensional processing is presented in Section 4 and examples of ambiguity function processing and spectral analysis are given in Sections 5 and 6.

II. TIME INTEGRATING CORRELATION

The one-dimensional time integrating correlator is reviewed. Consider the optical realization shown conceptually in Figure 1. The

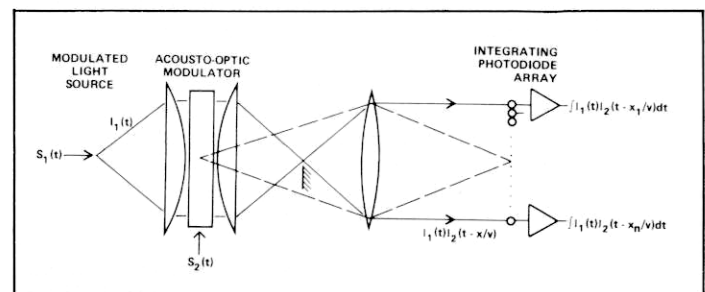


Figure 1. Time integrating correlator.

light source is temporally modulated by a signal, $s_1(t)$, to produce an output intensity $I_1(t)$, which illuminates an acoustic delay line light modulator. A second signal, $s_2(t)$, is introduced into the acoustic cell, which spatially modulates the source intensity by an amount denoted by $I_2(t - x/v)$, where x is the spatial dimension and v is the acoustic velocity. The acoustic signal is schlieren imaged onto a linear photodiode array; the intensity distribution in the image plane is given by the product $I_1(t)I_2(t - x/v)$. Distinction between coherent and noncoherent optical system implementation and interferometric versus noninterferometric detection will be described.

The charge integration, directly proportional to exposure, is performed by detectors at discrete positions, x_i . The resultant output voltage at the i^{th} detector element is therefore:

$$R_{12}(\tau_i) = \int_T I_1(t)I_2(t - x_i/v)dt \quad (1)$$

where $\tau_i = x_i/v$, and T , the integration time of the detector, is set by the timing of the charge transfer readout register. This is the desired correlation, where I_1 and I_2 are directly related to the input signals s_1 and s_2 . Several modulation/detection schemes may be employed in order to achieve a linear relationship.

The range of relative delay between input signals is limited by

the acoustic delay length, and the integration time is set by the detector readout period. The correlator time-bandwidth product, $B\tau$, may therefore be larger than the delay line time-bandwidth product, $B\tau$, since the integration time period may be longer than the acoustic delay. In spatial integrating correlators,¹⁶ the integration period is determined by the acoustic delay; in configurations employing fixed reference masks, the range of relative delay is unlimited, however, in correlators with acoustic reference, the range is limited to the acoustic delay. Long integration and flexibility of variable integration are achieved with the time integrating approach.

The achievable processing gain is limited by the correlator dynamic range which is determined by the detector dynamic range and the signal-to-bias ratio. The signal-to-bias ratio depends on the light intensity modulation depth. Detector dynamic range is limited by saturation and is defined as the ratio of saturation level to rms noise. The processing gain and dynamic range can be extended, however, by post-detection digital integration.

In all approaches to time integrating optical correlation, the goal is to achieve a term in the detected light intensity that is proportional to the product of the input signals. Acousto-optic devices modulate optical phase, thus are basically nonlinear modulators of electric field amplitude or intensity. However, linear electric field modulation is approximated at low diffraction efficiency (depth of phase modulation). Linear intensity modulation is approximated by operation with an optical bias at high diffraction efficiency ($\pi/4$ phase shift) and a small signal modulation depth. This latter technique has been exploited by Sprague and Koliopoulos.¹⁵ Interferometric detection may be used when acousto-optic modulation of electric field is linear. In one implementation, a coherent optical reference beam is used for interferometric detection. Another implementation is described that uses an electronic reference to realize interferometric detection with either coherent or noncoherent light. This approach is realized by adding a reference oscillator signal to the acoustic modulation, rather than using a reference beam with separate optical path. The basic difference between the coherent and noncoherent implementation is the spatial and temporal diversity of the illumination. Tolerance to angular and wavelength dispersion is determined by the acoustic diffraction and the Bragg condition. The magnitude transfer function, MTF, is related to the illumination and acoustic field by convolution of their angular spectrums.

In the interferometric schemes, it is assumed that acousto-optic modulation of the electric field is linearly proportional to the drive voltage, and that the imaging optics pass only the first diffraction order. This condition is approximated at low diffraction efficiency. Third order intermodulation may be in band and may contribute to the output. In special cases, these terms time-integrate to zero.

The implementation described uses an internally modulated diode source as shown in Figure 1. A reference oscillator signal is added to the acousto-optic deflector input with a frequency that is offset from the signal modulation; in addition the illumination source must be modulated on a carrier with equal frequency offset. Both single and double sideband modulation are analyzed.

The image intensity distribution, I , is given by the product of the source modulation, I_1 , and acousto-optic modulation denoted by $I_2 = |E_2|^2$ where E_2 is the complex electric field modulation.

$$I(t, x) = I_1(t)I_2(t - x/v). \quad (2)$$

For double sideband modulation

$$\begin{aligned} I_1(t) &= A_1[1 + \sqrt{2}m_1 s_1(t) \cos[2\pi f_0 t]] \\ E_2(t) &= A_2^{1/2}[1 + \sqrt{2}m_2 s_2(t)e^{j2\pi f_0 t}]e^{j2\pi f_c t} \\ I_2(t) &= |E_2(t)|^2 \\ &= A_2[1 + 2m_2^2 s_2^2(t) + 2\sqrt{2}m_2 s_2(t)\cos[2\pi f_0 t]], \end{aligned} \quad (3)$$

where f_0 is the frequency difference between the reference

oscillator at f_c and the double sideband suppressed carrier modulation at $f_c + f_0$. The +1 diffraction order is passed by the imaging optics. A_1 and A_2 correspond to light intensity and diffraction efficiency respectively; m_1 and m_2 are constants that determine the modulation depth. It is assumed that signals s_1 and s_2 are bandlimited to a bandwidth B (i.e., $|S(f)| = 0, |f| > B$), and have unit average power. The spectrum of the input modulation is shown in Figure 2. The device bandwidth is $f_0 + B$.

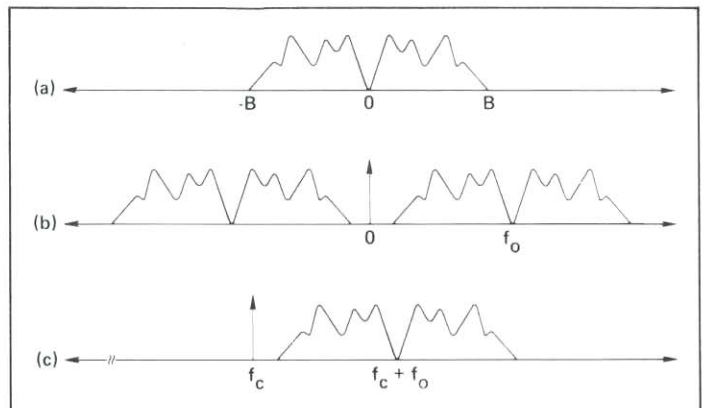


Figure 2. Spectrum of (a) input signal, (b) diode source modulation, and (c) acousto-optic deflector modulation for DSB example.

For $f_0 > 3B$ several cross terms effectively integrate to zero and the output becomes approximately:

$$\begin{aligned} R(\tau) &\approx A_1 A_2 \left\{ T + 2m_2^2 \cdot \int s_2^2(t - \tau) dt \right. \\ &\quad \left. + 2m_1 m_2 \cos[2\pi f_0 \tau] \cdot \int s_1(t) s_2(t - \tau) dt \right\} \end{aligned} \quad (4)$$

where $\tau = x/v$. The first two terms are bias and the last term is the desired correlation on a spatial carrier, f_0 . The bias terms may be eliminated through filtering. The ratio of signal-to-bias for maximum correlation is given by $\beta = 2m_1 m_2 / (1 + 2m_2^2)$.

For single sideband (SSB) modulation the bandwidth requirement is cut in half. The spectrum of the input modulation is shown in Figure 3. For $f_0 > 3/2 B$ the output correlation is approximately:

$$\begin{aligned} R(\tau) &\approx A_1 A_2 \left\{ \int dt + m_2^2 \left[\int s_2^2(t - \tau) + \tilde{s}_2^2(t - \tau) dt \right] \right\} \\ &\quad + 2m_1 m_2 (R_{12}(\tau) \cos[2\pi f_0 \tau] + \tilde{R}_{12}(\tau) \sin[2\pi f_0 \tau]) \end{aligned} \quad (5)$$

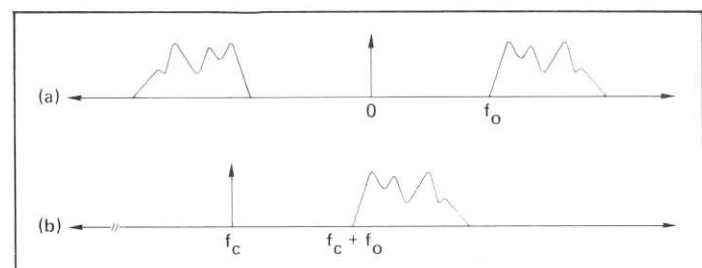


Figure 3. Spectrum of (a) diode source modulation, and (b) acousto-optic deflector modulation for SSB example.

where $R_{12}(\tau)$ is the desired correlation and \tilde{R}_{12} is the Hilbert transform of R_{12} ($\tilde{R}_{12} = R_{12}^H$). The desired correlation R_{12} may be synchronously detected.

Complex correlation using real computation is described in the following. In general, calculation of complex multiplication or correlation requires four real operations. Alternatively, frequency translation may be utilized to realize complex correlation with a single real correlator at the expense of bandwidth. The time inte-

grating spectrum analyzer described in the next section is an example of complex correlation by this method. Further advantage of correlation at a carrier frequency is the ability to filter the desired correlation from additional bias terms. The expressions for complex correlation are derived in the following.

Define the correlation between complex signals $x(t)$ and $y(t)$ by:

$$R_{xy}(\tau) = \langle x(t)y^*(t-\tau) \rangle \quad (6)$$

where

$$x(t) = x_R(t) + ix_I(t)$$

$$y(t) = y_R(t) + iy_I(t)$$

and $\langle \cdot \rangle$ denotes ensemble average.

$$\begin{aligned} \text{Re}\{R_{xy}(\tau)\} &= \langle x_R(t)y_R(t-\tau) \rangle + \langle x_I(t)y_I(t-\tau) \rangle \\ \text{Im}\{R_{xy}(\tau)\} &= -\langle x_R(t)y_I(t-\tau) \rangle + \langle x_I(t)y_R(t-\tau) \rangle. \end{aligned} \quad (7)$$

Consider the real correlation between $x_0(t)$ and $y_0(t)$,

$$\begin{aligned} R_{x_0y_0}(\tau) &= \langle x_0(t)y_0(t-\tau) \rangle \\ x_0(t) &= \text{Re}\{x(t)e^{j2\pi f_0 t}\} \\ y_0(t) &= \text{Re}\{y(t)e^{j2\pi f_0 t}\} \end{aligned} \quad (8)$$

where $x(t)$ and $y(t)$ are bandlimited with bandwidth B , and $f_0 > B$.

$$R_{x_0y_0}(\tau) \approx \frac{1}{2} \text{Re}\{R_{xy}(\tau)e^{j2\pi f_0 \tau}\}. \quad (9)$$

Cross products at the sum frequency $2f_0$ average to zero for $f_0 > B$. Thus, the correlation between x_0 and y_0 is at a carrier frequency f_0 , with carrier phase modulated by the phase of R_{xy} , and envelope equal to the magnitude of R_{xy} . The real and imaginary parts of $R_{xy}(\tau)$ may be derived from $R_{x_0y_0}$ by synchronous detection (in quadrature).

III. TIME INTEGRATING SPECTRAL ANALYSIS

An approach to real time optical spectral analysis of electrical signals that uses a time integrating, rather than spatial integrating, version of the chirp z-transform, is described. The large time-bandwidth correlation is accomplished by means of the correlator described in the previous section. A time integrating architecture for correlation and spectral analysis, using oppositely traveling acoustic waves, has been described by Montgomery.¹⁴ For time integrating realizations, frequency resolution is determined by the detector integration period, rather than the acoustic delay length, therefore, higher resolution can be achieved than by spatial integration. Variable resolution is attainable through variable time integration. Use of intensity modulation leads to detection of the magnitude spectrum rather than the power spectrum which yields a considerable increase in dynamic range. This approach to spectral analysis achieves a flexibility not readily achieved by coherent optical spatial methods. The chirp algorithm,^{17,18} is reviewed, and the real implementation is discussed.

The Fourier transform integral

$$S(f) = \int s(t)e^{-j2\pi ft} dt \quad (10)$$

may be rewritten as

$$S(f) = e^{-j\pi f^2} \int s(t)e^{-j\pi t^2} e^{j\pi(t-f)^2} dt, \quad (11)$$

by expressing $f \cdot t$ as $\frac{1}{2}[f^2 + t^2 - (t-f)^2]$. The complex realization is shown in Figure 4. The post-phase weighting may be ignored if only the magnitude or power spectrum is required. This realization

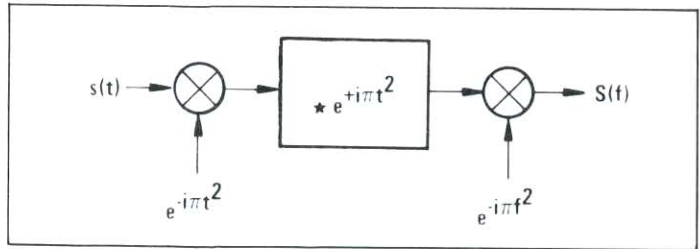


Figure 4. Complex realization of chirp algorithm.

converts the integral transform to time invariant filtering of a preweighted signal, followed by post-weighting.

The chirp algorithm may be realized with a single real correlation by translating the real chirp to a carrier frequency, f_0 , greater than the signal analysis bandwidth, B . The desired difference frequency is translated to baseband, and the sum frequency is an out-of-band chirp that integrates to zero. The product of the difference frequency, which is a linear function of delay, and the input signal, is integrated, producing the Fourier transform. The magnitude spectrum corresponds to the detected envelope. The phase modulates the spatial carrier and may be detected as well, resulting in a complex output.

Frequency resolution of this spectrum analyzer is inversely proportional to the detector integration time, T . The resolution is *not* set by the acoustic time delay which typically limits the use of acousto-optical processing to wideband analysis. A wide range of integration times are easily realized (0.1-100 msec) using self-scanned arrays of moderate size (e.g., 1024). Integration time periods can be extended by means of electronic accumulation.

The delay line length, τ , and the number of detectors, N , set the delay, $\Delta\tau$, between detector elements in the image plane. This determines the chirp bandwidth B' . The required resolution or integration period fixes the chirp rate, α , (see Figure 5). The spatial

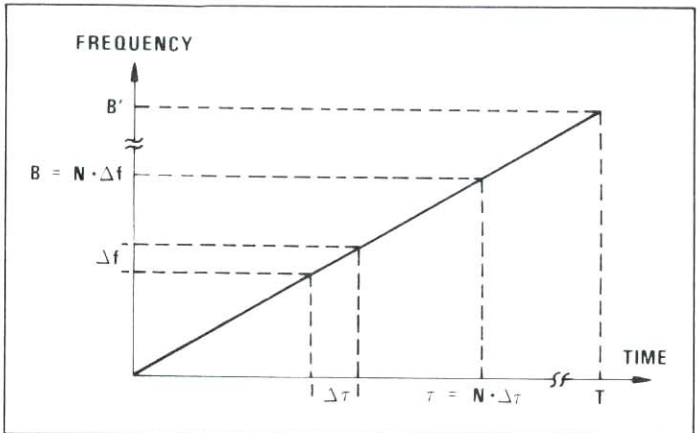


Figure 5. Instantaneous frequency of chirp.

bandwidth equals the chirp bandwidth, B' , plus carrier frequency, f_0 . Let k be the number of samples (detectors) per cycle of the highest frequency ($k = 2$ for Nyquist sampling), and define k' as the ratio of frequency offset to chirp bandwidth, f_0/B' . The above relationships may be written as:

$$\begin{aligned} N &= k(f_0 + B')\tau \\ \alpha &= B'/T = B/\tau \\ k' &= f_0/B' \geq 1. \end{aligned} \quad (12)$$

The time-bandwidth product is, therefore

$$BT = N/k(1+k') < N/4. \quad (13)$$

The dynamic range is limited by detection noise. If there are M distinguishable levels in the output voltage between the noise floor and the photo element saturation value, and if β is the maximum ratio of signal-to-bias, then the dynamic range in dB is given by $20 \log_{10} M\beta/(1+\beta)$, since incident exposure is directly proportional to spectral magnitude. This results in a considerable increase in dynamic range as compared to coherent optical power spectral analysis in which incident exposure is related to spectral power density and the dynamic range is given by $10 \log_{10} M$.

An experimental breadboard was constructed using a non-coherent implementation with a light emitting diode source. The modulation was double sideband and the chirps had octave bandwidth ($k'=1$). The correlator output for a sine wave input is shown in Figure 6. In this photograph the envelope is observed since the

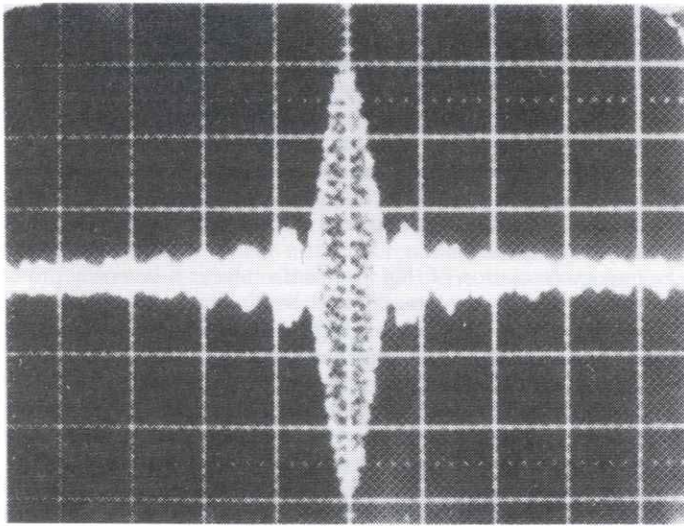


Figure 6. Time integrating spectrum analyzer output.

exposure covers multiple integration periods in which the signal phase is changing. Parameters of this example were: $N = 1000$, $\tau = 40 \mu\text{sec}$, $B' = 2.5 \text{ MHz}$, $T = 2 \text{ msec}$, $BT = 100$, $k = 5$, $k' = 1$. The signal-to-bias ratio, β , was 20% and the detector dynamic range (peak to rms) was $M = 1000$. The dynamic range observed was 40 dB ($\beta M/2$) since the bias was set at $M/2$ rather than optimized at $M/(1+\beta)$. The dynamic range is 3 dB greater using SSB input modulation.

IV. TWO-DIMENSIONAL PROCESSING

Two-dimensional integral transforms, for which the kernel is decomposable in the proper way, may be implemented by time integrating optical processing. Two important examples are ambiguity plane processing and spectral analysis.

Consider the optical realization shown conceptually in Figure 7. The optical train has a modulated illumination source, two acoustic delay line light modulators, and a matrix array of detectors. This configuration may be employed for several functions, determined by input signal and reference waveforms. It is assumed throughout this discussion that two-dimensional processing is applied to either very long one-dimensional signals or to two-dimensional signals (e.g., imagery) that are in raster format. In this way, the input will be a function of one variable, t ; the output $R(\tau_1, \tau_2)$ is a function of two variables.

The light diffracted by the first acousto-optic modulator A01, is diffracted by the second, A02, in an orthogonal direction. Both acoustic signals are imaged on the detector plane. The desired image plane intensity distribution has a term proportional to the product of acoustic signals, $s_1(t-\tau_1)s_2(t-\tau_2)$, where $\tau_1 = y/v$ and $\tau_2 = x/v$ are time variables. The resultant detected output voltage is proportional to the integrated charge as in the previously described

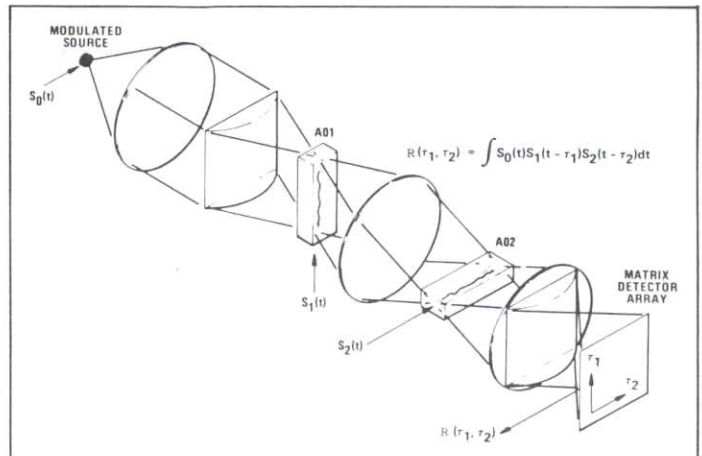


Figure 7. Two-dimensional time integrating optical processor.

correlator. This structure implements integrals of the form:

$$R(\tau_1, \tau_2) = \int_I s_0(t)s_1(t-\tau_1)s_2(t-\tau_2)dt . \quad (14)$$

In this configuration, all signals are real. In order to perform complex computation, similar considerations apply that were given for one-dimensional processing.

Hybrid realizations that use a combination of spatial and time integration can be used to implement a variety of other operations. An example of spectral analysis utilizing spatial integration for coarse resolution and time integration for fine resolution is described by Bader.¹⁹

The two-dimensional time integrating optical processor may be implemented with several modulation/detection schemes. A description of a coherent optical implementation using an interferometric optical reference has been given by Turpin.⁵ Non-coherent implementation using an intensity modulated light emitting diode offers immunity to noise suffered in coherent imaging. Noncoherent optical implementation using a reference oscillator for interferometric detection may be used to realize complex operation. Input modulation must be designed such that undesired terms are out of band.

The next examples demonstrate the strength of two-dimensional time integrating processors.

V. AMBIGUITY FUNCTION PROCESSING

Ambiguity function processing is important in resolution of delay and Doppler uncertainty. In application to radar signal processing or external signal parameter measurement, delay and Doppler are often time-varying. An ambiguity function snapshot is therefore desirable. A noncoherent optical parallel processing implementation for achieving such a snapshot is given in this section.

This example utilizes the 2-D optical system shown in Figure 7 which was generalized in the last section. The cross ambiguity function between complex signals $x(t)$ and $y(t)$ may be defined as

$$A_{xy}(\tau, f) = \int_0^T x(t)y^*(t-\tau)e^{-j2\pi ft} dt \quad (15)$$

where the variables τ and f may be interpreted as delay and Doppler, respectively. A real implementation of the complex cross-ambiguity function is described that uses the architecture of Section 4. The spectral analysis operation is performed using the chirp algorithm. Complex correlation was derived in Section 2 and is easily extended to two-dimensional computation.

Define the complex input signals $s_0(t)$, $s_1(t)$, and $s_2(t)$ by

$$s_0(t) = x(t)e^{-j\alpha\pi t^2}$$

$$\begin{aligned} s_1(t) &= y^*(t) \\ s_2(t) &= e^{j\alpha\pi t^2}, \end{aligned} \quad (16)$$

and consider the interferometric implementations of Section 2 with electronic reference. In the case of complex inputs, the intensity modulation is given by

$$\begin{aligned} I_0(t) &= A_0 [1 + \sqrt{2}m_0 \operatorname{Re}\{s_0(t)e^{j2\pi f_0 t}\}] \\ I_1(t) &= A_1 [1 + 2m_1 |s_1(t)|^2 + 2\sqrt{2}m_1 \operatorname{Re}\{s_1(t)e^{j2\pi f_1 t}\}] \\ I_2(t) &= A_2 [1 + 2m_2 |s_2(t)|^2 + 2\sqrt{2}m_2 \operatorname{Re}\{s_2(t)e^{-j2\pi f_2 t}\}] \end{aligned} \quad (17)$$

where double sideband modulation is assumed. The integrated intensity, $R(\tau_1, \tau_2)$,

$$R(\tau_1, \tau_2) = \int_0^T I_0(t)I_1(t-\tau_1)I_2(t-\tau_2)dt \quad (18)$$

contains the desired ambiguity function term,

$$\operatorname{Re}\{A_{xy}(\tau_1, \alpha\tau_2)e^{-j[2\pi(f_1\tau_1 - f_2\tau_2) + \alpha\pi\tau_2^2]}\}, \quad (19)$$

which is at a carrier frequency and may be filtered from other cross-product terms. The quadratic phase term may be cancelled through post-detection weighting. The variables τ_1 and τ_2 correspond to delay and Doppler respectively. The Doppler resolution is commensurate with the integration time; the analysis bandwidth is determined by Eq. (13). A coarse resolution may be maintained during a signal acquisition period, and a higher resolution zoom can be achieved by longer integration. Multiple correlation peaks or targets can be processed simultaneously since a linear system implementation is used.

Ambiguity function processing was demonstrated using the noncoherent optical implementation shown in Figure 7. Devices included a Hitachi HLP-20 light emitting diode, Fairchild SL62926 charge coupled device image sensor, and Isomet acousto-optic devices. The diode has a 30 MHz 3 dB bandwidth and was biased at an average optical power of approximately 10 mW. The image sensor has 380×488 elements and was operated with an integration period of 33.34 msec. The acousto-optic devices have a 30 MHz 1 dB bandwidth and 50 μ sec delay. Chirp waveforms of very large time-bandwidth product ($BT \leq 2^{19} = 524,288$) were synthesized digitally. The delay range was limited to $36 \times 27 \mu$ sec (4:3 aspect ratio) to increase the signal bandwidth. The image plane sampling was, therefore, $380 \div 36 \mu$ sec $\cong 10.6$ MHz in one delay dimension and $488 \div 27 \mu$ sec $\cong 18.1$ MHz in the other dimension. The overall system frequency response (MTF) was approximately 3 dB lower at the Nyquist limit (2 samples per cycle) 5 and 9 MHz, respectively. An example ambiguity function of a short pseudo-random code is shown in Figure 8. The Doppler range was 1.3-5 kHz determined by the chirp rate. The code repetition period was 6.2 μ sec (31 length, 5 MHz rate), therefore, 4 correlation peaks are evident in the ambiguity function; the Doppler was 2 kHz. The time bandwidth product was $5 \text{ MHz} \times 33.34 \text{ msec} = 166,700$. No post-detection processing has been applied to the output video. A signal dependent bias variation, proportional to the pairwise cross-correlations between inputs, has not been filtered. The image has several blemishes due to the CCD camera. The sensor dynamic range is approximately 60 dB, and the maximum signal-to-bias ratio was 25%; the resultant input signal dynamic range was, therefore, 48 dB.

VI. SPECTRAL ANALYSIS

A noncoherent optical time integrating approach to two-dimensional complex spectral analysis is described. This method is an extension of the technique described for one-dimensional

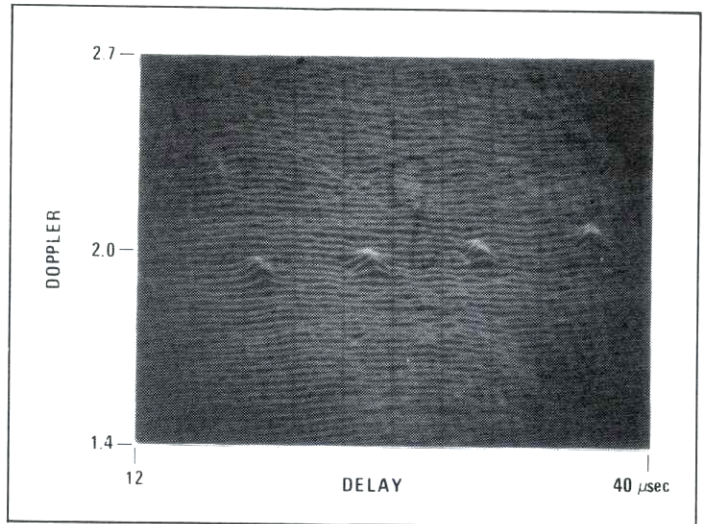


Figure 8. Ambiguity function for short code.

analysis. Very large time-bandwidth (greater than 10^5) spectral analysis of electrical signals can be performed using this time domain approach, without requiring storage of the signal. Spectral analysis of raster scanned video imagery can be performed as well.

The optical system (Figure 7) described in the last sections is used in this example as well. The algorithm is implemented with three reference chirp waveforms. The source is modulated with the input signal, which is premultiplied by a chirp, and the other chirps modulate A_0 and A_2 . The chirp rates are chosen such that the product of the three chirps result in a temporal sine wave, with frequency that is varying from pixel to pixel on the detector array. Each detector element integrates the product of this sine wave times the input signal, and, in this fashion, produces the spectrum. The frequency difference between output lines in one dimension is taken to be N times the frequency difference between lines in the other dimension, where N is the number of detectors per line. For a square array, the number of spectral samples is proportional to N^2 . The technology is currently limited by detector array size, and detector readout rate.

A two-dimensional chirp algorithm with three complex reference chirps is described next. The real implementation is performed with frequency offset chirps, similar to the previous examples. Define the transform (optical processor output) by

$$R(\tau_1, \tau_2) = \int_{-NT/2}^{NT/2} s(t)a(t)b(t-\tau_1)c(t-\tau_2)dt \quad (20)$$

where

$$\begin{aligned} a(t) &= \sum_n e^{-j\alpha\pi(t-nT)^2} \operatorname{rect}\left(\frac{t-nT}{T}\right) \\ b(t) &= e^{j\alpha\pi t^2/N} \operatorname{rect}(t/NT) \\ c^*(t) &= a(t) b(t). \end{aligned} \quad (21)$$

Waveforms $a(t)$ and $c(t)$ are periodic chirps with period T and chirp rates α and $\alpha(N-1)/N$, respectively. Waveform $b(t)$ is a low rate chirp with period NT and rate α/N . The chirp rates are chosen such that a constant difference frequency, $f = \alpha[\tau_1 + (N-1)\tau_2]/N$, is generated by the product $a(t)b(t-\tau_1)c(t-\tau_2)$. Frequency discontinuities occur during intervals $nT < t < nT + \tau_2$ due to the chirp transition traversing the acoustic delay aperture. This effectively reduces the integration time by the factor $(T-\tau_2)/T$. However, this may be completely compensated by increasing the chirp bandwidth. This effect is ignored in the following analysis, thus

$$a(t)b(t-\tau_1)c(t-\tau_2) \approx$$

$$\sum_n e^{j[2\pi\alpha n T \tau_2 - 2\pi\alpha t[\tau_1 + (N-1)\tau_2]/N + \phi(\tau_1, \tau_2)]} \cdot \text{rect}\left(\frac{t-nT}{T}\right) \text{rect}\left(\frac{t}{NT}\right) \quad (22)$$

where

$$\phi(\tau_1, \tau_2) = \alpha\pi[\tau_1^2 + (N-1)\tau_2^2]/N.$$

The spectral phase weighting, $\phi(\tau_1, \tau_2)$ may be compensated post-detection. Equation (20) becomes

$$R(\tau_1, \tau_2) = e^{j\phi} \int NT \text{sinc}(Tf) S[f - \alpha[\tau_1 + (N-1)\tau_2]/N] \cdot \sum_n \text{sinc}[NT(f + \alpha\tau_2 - n/T)] df. \quad (23)$$

As evidenced by the term $S[\alpha(\tau_1 + (N-1)\tau_2)/N]$, the variables τ_1 and τ_2 may be interpreted as fine and coarse frequency, respectively. Integration over N chirp repetitions has created a comb sampling along the coarse frequency axis, with comb samples a function of the fine frequency axis. The spectral resolution is proportional to $1/NT$ where NT is the total integration period.

VII. SUMMARY

Time integrating optical techniques for one- and two-dimensional complex signal processing have been described. Signal processing architectures utilizing actively generated reference waveforms such as chirps realize a wide range of algorithms and variable time integration allows further flexibility. Particularly attractive is the multipurpose capability of the time integrating optical processor, e.g., the same optical system is used for both spectral analysis and ambiguity function processing.

The technique of interferometric detection with electronic reference was described. In this implementation, a local oscillator is added to the acoustic modulation rather than a coherent optical reference added to the image. This method, therefore, permits non-coherent optical implementation, with the advantages of directly modulated diode light sources and increased immunity to artifacts of coherent optical imaging systems. The correlation is performed at a carrier, thereby enabling complex operation. Furthermore, the interferometric method circumvents the difficult requirement for acoustic modulation at a high diffraction efficiency bias point, that is necessary for linear operation in the noninterferometric technique.

The optical implementation, utilizing acousto-optic input and integrating image sensor output devices, creates a processor that is highly compatible with signal processing systems. Such implementation affords very large time-bandwidth product signal processing without the input signal storage requirement associated with spatial integrating methods. The requirement for high resolution, large dynamic range output image sensors becomes the key device limitation. Acousto-optic devices are available with time-bandwidth product much greater than the number of resolvable image samples.

The key attributes of time integrating techniques are summarized in the following: extremely large time-bandwidth correlations may be performed, independent of the device time-bandwidth product; a flexible, multipurpose processor is realized by use of actively generated reference waveforms and variable time integration; an important class of two-dimensional algorithms, including complex spectral analysis and ambiguity function processing, may be performed without having to store the entire time history as a spatial record; the system may be implemented with noncoherent diode sources, acousto-optic devices, and integrating image sensors.

ACKNOWLEDGMENT

The author acknowledges funding support by ESL, Incorporated under the Internal Research and Development program and by the Air Force Office of Scientific Research under contract F49620-78-C-0102.

REFERENCES

1. L. J. Cutrona, E. N. Leith, C. J. Palermo, and L. J. Porcello, "Optical Data Processing and Filtering Systems," *IRE Trans. Info. Theory*, Vol. IT-6, pp. 386-400, June 1960.
2. J. W. Goodman, "Operations Achievable with Coherent Optical Information Processing Systems," *Proc. IEEE*, Vol. 65, pp. 29-38, January 1977.
3. P. Kellman, "Detector Integration Acousto-Optic Signal Processing," *Proc. Int. Optical Computing Conf.*, London, England, pp. 91-95, September 1978.
4. P. Kellman, "Time Integrating Optical Processors," *Optical Processing Systems*, Proc. Soc. Photo-Opt. Instr. Eng. 185, 130-139 (1979).
5. T. Turpin, "Time Integrating Optical Processors," *Real-Time Signal Processing*, Proc. Soc. Photo-Opt. Instr. Eng. 154, 196-203 (1978).
6. C. Skenderoff, et al., "Radar Receiver Having Improved Optical Correlator Means," U.S. Patent 3 483 557, December 1969.
7. A. J. Talamini, Jr. and E. C. Farnett, "New Target for Radar: Sharper Vision with Optics," *Electronics*, Vol. 38, pp. 58-66, December 1965.
8. J. K. Parks, "Optical Correlation Detector for the Audio Frequency Range," *J. Acoust. Soc. Amer.* 37, 268-277 (1965).
9. K. Bromley, "An Optical Incoherent Correlator," *Opt. Acta* 21, 35-41 (1974).
10. M. A. Monahan, R. P. Bocker, K. Bromley, and A. Louie, "Incoherent Electro-Optical Processing with CCD's," in *Dig. Int. Optical Computing Conf.* (Washington, DC) (IEEE Catalog 75 C40941-5C), April 1975.
11. M. Arm, M. King, A. Aimette, and L. B. Lambert, in *Proceedings of the Symposium on Modern Optics*, F. Fox, Ed. (Polytechnic Press, Brooklyn, NY, 1967), pp. 691-702.
12. J. W. Goodman, "Temporal Filtering Properties of Holograms," *Appl. Optics* 6, 857-859 (1967).
13. R. W. Ralston, D. H. Hurlburt, F. J. Leonberger, J. H. Cafarella, and E. Stern, "A New Signal-Processing Device, The Integrating Correlator," 1977 Ultrasonics Symposium Proceedings, New York, pp. 623-628.
14. R. M. Montgomery, "Acousto-Optical Signal Processing System," U.S. Patent 3 634 749, January 1972.
15. R. A. Sprague and C. L. Koliopoulos, "Time Integrating Acousto-Optic Correlator," *Appl. Optics* 15, 89-92 (1976).
16. R. Sprague, "A Review of Acousto-Optic Signal Correlators," *Optical Engineering* 16, 467-474 (1977).
17. L. R. Rabiner, R. W. Schafer, and C. M. Rader, "The Chirp Z-Transform Algorithm and Its Application," *Bell System Technical Journal*, pp. 1249-1292, May-June 1969.
18. H. J. Whitehouse, R. W. Means, and J. M. Speiser, "Signal Processing Architectures Using Transversal Filter Technology," *Proceedings of the IEEE Symposium on Circuits and Systems*, Boston, April 1975.
19. T. R. Bader, "Coherent Optical Hybrid Techniques for Spectrum Analysis," *Optical Processing Systems*, Proc. Soc. Photo-Opt. Instr. Eng. 185, 140-146 (1979). ©